Received: 11 June 2020 | Accepted: 9 October 2020

DOI: 10.1002/saj2.20174

Soil Science Society of America Journal

SOIL PHYSICS & HYDROLOGY

Limiting water range: Crop responses related to in-season soil water dynamics, weather conditions, and subsoil compaction

Mansonia Pulido-Moncada[1] | **Carsten T. Petersen**[2] | **Lars J. Munkholm**[1]

[1] Dep. of Agroecology, Research Centre Foulum, Aarhus Univ., Blichers Allé 20, P.O. Box 50, Tjele DK-8830, Denmark

[2] Dep. of Plant & Environmental Sciences, Univ. of Copenhagen, Thorvaldsensvej 40, Frederiksberg 1871, Denmark

Correspondence
Lars J. Munkholm, Dep. of Agroecology, Research Centre Foulum, Aarhus Univ., Blichers Allé 20, P.O. Box 50, Tjele DK-8830, Denmark.
Email: lars.munkholm@agro.au.dk

Abstract

The least limiting water range (LLWR) has been used as a soil structural quality indicator for identifying in-season water dynamics, yet studies focusing on its use for detecting in-season water stresses and their effect on crop response on severely compacted subsoils are scarce. The objectives of this study were, therefore, to examine the in-season water dynamics on a tile-drained soil with compacted subsoil in the light of two different approaches for calculating LLWR (standard LLWR by da Silva et al. [1994] and refined LLWR by Pulido-Moncada & Munkholm [2019]) and to evaluate the crop response to aboveground and belowground conditions. Information on LLWRs was obtained from soil sampling in the most contrasting treatments of a compaction experiment: with and without compaction. In-season water dynamics were measured from 2017 to 2019. The refined LLWR approach defined a wider range of water content nonlimiting for plant growth compared with the da Silva et al. approach. Compaction affected the LLWRs ($p < .05$), yet no significant effect of subsoil compaction on crop yield was found. Cumulative aeration and water stress day indicators identified from the refined LLWR were significantly related to grain yield ($p < .05$). The lower winter wheat yield in 2018 compared with 2019 seemed to be related to the direct impact of weather factors on aboveground growth and to aeration and water stresses. The apparent lack of compaction effect suggests further studies are needed to determine if in-season stresses derived from the LLWRs can be related to crop development and yield under different soil and weather conditions.

1 | INTRODUCTION

Soil structure conditions govern plant root development because they affect the air, water, and nutrient distribution in the soil matrix and determine the force the roots might need to penetrate and propagate downward (Bengough et al., 2006). Under conventional tillage with heavy traffic, the subsoil is commonly characterized by compacted layers with a massive structure (Ball et al., 2015). Topsoil and subsoil compaction have been found to have a different accountability degree on crop response, with a varying persistency effect in clay loam soils (Håkansson & Reeder, 1994). In coarse-textured soils that are annually plowed, subsoil compaction effects may persist longer or be permanent (Alakukku, 1996; Berisso et al., 2012). Studies are needed to quantify the subsoil compaction effect on crop yields after the termination of heavy annual traffic.

Abbreviations: ASD, aeration stress day; FC, field capacity; LLWR, least limiting water range; PR, penetration resistance; RAW, readily available water; RVI, relative vegetation index; WP, permanent wilting point; WSD, water stress day.

Soil compaction involves a number of soil physical stresses that narrow the range of water content at which there are minimal physical limitations to root growth (Chen, Weil, & Hill, 2014). This water content approach was introduced as the least limiting water range (LLWR) by da Silva, Kay, and Perfect (1994), which is a modification of that proposed by Letey (1958) and integrates the relationship between the water content at the critical values of water potential, mechanical resistance, and aeration.

The LLWR has been used for identifying the limiting factors for plant growth under different tillage systems (Betz, Allmaras, Copeland, & Randall, 1998; Kahlon & Chawla, 2017; Tormena, da Silva, & Libardi, 1999) and soil management and land use (Calonego & Rosolem, 2011; Fidalski, Tormena, & Silva, 2010; Gonçalves et al., 2014; Reichert, da Silva, & Reinert, 2004), including forest soils (Sato, Lima, Ferreira, Rodrigues, & Silva, 2017; Zou, Sands, Buchan, & Hudson, 2000). The estimated da Silva et al. (1994) LLWR values for topsoil conditions have been found to be related to crop yield (Beutler et al., 2008; Beutler, Centurion, & Silva, 2005; Lapen, Topp, Gregorich, & Curnoe, 2004). However, the limits of the LLWR proposed by da Silva et al. (1994) have been argued by other authors. For the upper limit, field capacity (FC) and 10% of air-filled porosity are considered too simplistic estimations of aeration status because they do not take soil pore organization into account (Kadžienė, Munkholm, & Mutegi, 2011; Lapen et al., 2004; Mohammadi, Asadzadeh, & Vanclooster, 2010; van Lier & Gubiani, 2015). For the lower limit, a fixed penetration resistance (PR)-based limit does not consider the root penetration capability of the plant species at high PR levels as well as the ability to grow through preferential pathways such as biopores and cracks (Bengough & Mullins, 1990; Whitmore & Whalley, 2009). The permanent wilting point (WP), which is the second expression of the lower limit of the da Silva et al. (1994) approach, is considered an ultimate limit that does not take into account the reduction in transpiration as the soil dries (Silva et al., 2015).

Although the da Silva et al. (1994) LLWR approach might be still in development, a refinement in relation to the complexity of the boundaries conditions was proposed by Pulido-Moncada and Munkholm (2019). They suggested the use of the water content at a critical value of relative gas diffusivity as the upper limit (Kadžienė et al., 2011) and the critical soil water content at which a reduction in stomata opening occurs as the lower limit (Silva et al., 2015). These, respectively, represent the soil water state at which there is no restriction for gas transport (Kadžienė et al., 2011) and at which plants can extract water without suffering water stress (Silva et al., 2015).

da Silva and Kay (1996) suggested identifying the periods when the soil water content is outside the LLWR, which may be proportionally related to crop growth and yield. The LLWR has subsequently been used in other studies to evaluate the stresses suffered by the crop during a growing season (Bengough et al., 2006; Klein & Camara, 2007; Silva et al., 2019). However, apparent water stress in the topsoil may not be expressed when there is available water in deeper soil layers (Silva et al., 2019). In compacted soils, the penetration of roots to deeper soil layers may not occur uniformly (Taylor & Brar, 1991) because the ability of roots to penetrate hard layers depends on species-specific mechanisms (Lynch & Wojciechowski, 2015).

On the other hand, aboveground factors during the growing season may rule plant growth and productivity when water and nutrient uptake is sufficient (Qin, Noulas, & Herrera, 2018; Shah & Paulsen, 2003). Meteorological stresses have a negative effect on crop yield depending on the plant species or cultivar grown because grain and seed crops are more sensitive than others (Peltonen-Sainio et al., 2010). Harmful effects of, for example, low or high temperatures at critical development stages such as heading and anthesis cannot be compensated for by optimal subsequent conditions (Mäkinen et al., 2018). Although crop response to heat stress is known to be more dramatically marked by drought stress (Alghabari, Lukac, Jones, & Gooding, 2014), high air temperature can reduce water-use efficiency even when plants are not stressed for soil moisture (Shah & Paulsen, 2003).

Taking into account the combined effect of different stresses during the crop life cycle, and particularly the effect of severely compacted subsoil, is crucial to identifying yield-related in-season stresses. Nevertheless, studies evaluating the relation between in-season stresses, crop response, and LLWR are scarce. The present study aims (a) to evaluate the residual effect of subsoil compaction for a tile-drained sandy loam on the LLWR, (b) to examine the in-season water dynamics in the light of two LLWR approaches, and (c) to evaluate the crop response to aboveground and belowground conditions. It was hypothesised (a) that subsoil compaction would narrow the LLWRs and reduce crop yields and (b) that yield effects could be related to the extent of aeration and/or water stress derived from soil water contents outside the LLWRs.

Core ideas

- Available water limits allowed the identification of in-season water stresses.
- Residual subsoil compaction affected aeration stress but not wheat grain yield.
- Aeration and water stress periods were correlated with wheat grain yield.

TABLE 1 Field operations in the experimental trial for 2017–2019

	2017	2018	2019
Crop	**Spring barley**	**Winter wheat**	**Winter wheat**
Catch crop sown (+30N)	13 Aug. 2016		
Ploughing	11 Nov. 2016	29 Sept. 2017	21 Sept. 2018
Sowing	3 Apr. 2017	30 Sept. 2017	21 Sept. 2018
Fertilization	3 Apr. 2017	9 Apr. 2018[a]	26 Mar. 2019[b]
Fertilizer, kg N ha^{-3}	110	147	152
Harvesting	16 Aug. 2017	30 July 2018	5 Aug. 2019

[a]41 kg N (9 Apr.) + 20 kg (12 Apr.) + 86 kg N (20 Apr.).
[b]84 kg N (26 Mar.) + 68 kg (15 Apr.).

2 | MATERIALS AND METHODS

2.1 | Study site and compaction experiment

The study was conducted in a compaction experiment located at the Taastrup Research Centre (55°40′43″ N, 12°16′43″ E) of Copenhagen University, Denmark. The soil at Taastrup is a sandy loam soil developed on moraine deposits from the Weichselian glaciation. The 0-to-0.25 m soil layer contained 197, 285, and 518 g kg^{-1} of clay (<2 μm), silt (2–63 μm), and sand (63 μm–2 mm), respectively, and 25 g kg^{-1} of soil organic matter. Corresponding values at the 0.25-to-0.50-m depth are 233, 287, 480, and 12 g kg^{-1}, respectively, and at the 0.50-to-1.0-m depth are 239, 312, 449, and 5 g kg^{-1}, respectively.

The compaction experiment at Taastrup consisted of an annual heavy traffic event with slurry application machinery during the period 2010–2013. The experimental traffic took place at a water content close to FC on plowed soil in spring. In the present study, the most contrasting experimental treatments were selected: control soil that underwent no experimental traffic and compacted soil that consisted of five passes of a tractor–slurry trailer combination with ~58-kN wheel load. The experimental treatments were arranged in a randomized complete block design with four blocks.

When sampling, in spring 2017, the subsoil (0.3 m depth) of the compacted plots was characterized by a significantly higher soil bulk density (1.77 Mg m^{-3}) and lower air-filled porosity (0.06 m^3 m^{-3}) and gas diffusivity (0.0034) compared with the control treatment (1.62 Mg m^{-3}, 0.10 m^3 m^{-3}, and 0.0084, respectively) (Pulido-Moncada, Schjønning, Labouriau, & Munkholm, 2020). Further details on the experimental field, treatments, and results of soil physical parameters during the compaction experimental years and after completion of the compaction experimental period have been reported in previous studies (Pulido-Moncada & Munkholm, 2019; Pulido-Moncada et al., 2020; Schjønning, Lamandé, Crétin, & Nielsen, 2017; Schjønning, Lamandé, Munkholm, Lyngvig, & Nielsen, 2016).

The soil in the experimental trial was annually plowed to approximately 0.25 m in autumn from 2016 to 2019. After shallow secondary tillage, spring barley (*Hordeum vulgare* L.) was sown annually in spring from 2010 to 2017. In 2017 and 2018, winter wheat (*Triticum aestivum* L.) 'Sheriff' was sown in late September. Details of the field operations are presented in Table 1.

2.2 | Meteorological data

Meteorological data were obtained from the climate and water balance station located at Taastrup, 1.5 km from the experimental site. Weather data, including daily mean temperature and precipitation, were measured during the growing seasons for the 3 yr of evaluation (i.e., 2017–2019). Reference evapotranspiration was calculated on a daily basis by the Penman equation (Penman, 1948).

2.3 | Soil water content measurement

Water contents were measured at different soil depths from 0.1 to 1.0 m and at different dates from 2017 to 2019 with a multisensor capacitance PR2 Profile Probe (Delta-T Devices Ltd). Built-in standard calibration for mineral soil was used so that water content could be logged directly.

Similar to most agricultural fields on loamy soil in Denmark, the experimental field in Taastrup is tile drained (Møller, Beucher, Iversen, & Greve, 2018; Olesen, 2009). Typically, such fields will have a perched water table in the root zone during the drainage season in autumn-winter and at the drain depth at the beginning of April when net precipitation becomes negative. Therefore, water content measurements were conducted from April to July during the 3 yr

of evaluation. In 2017, water content was measured 13 times between 30 April and 17 July; in 2018, 17 times between 9 April and 29 June; and in 2019, 18 times between 3 April and 30 June. In 2018, the access tubes were installed shortly after tillage in autumn. Because of soil settlement in the plow layer during autumn and winter, in-season measuring depths were slightly different this year, and the measuring depths differ by 0.05 m on average.

2.4 | Field PR measurements

In 2017, 4 yr after completion of the compaction experiment, field PR was measured directly in the field in November, at a soil water content near FC, with the help of an automated cone penetrometer (Olsen, 1988). Within each experimental plot, 10 measurements down to 0.80 m depth were conducted. Measurements were recorded at 10-mm increments with a 20.27-mm-diameter cone with a 30° semi-angle tip and at a penetration speed of 30 mm s^{-1}.

In this study, because the topsoil of both control and compacted treatments was plowed annually (~0.25 m) and hence is characterized by a homogenous structural arrangement (as shown below), we further focused on two layers of the subsoil: the 0.3-m and the 0.6-m depth. These layers represent the most compacted layer and the layer below the compacted layer, respectively.

2.5 | Sampling and laboratory measurements

Sampling of 100-cm^3 soil cores (0.061 m in diameter and 0.035 m in height) was conducted at 0.3 m depth. Within each of the four trial blocks, six replicate cores were collected at each of the three selected sampling spots. The soil cores were kept at 2 °C until analysis.

Sequential measurements of air-filled porosity (ε_a) and relative gas diffusivity (D_s/D_o) were conducted for all the soil cores after water content was equilibrated at −100 hPa matric potential on tension tables. The ε_a was measured by using an air pycnometer (Flint & Flint, 2002; Rüegg, 2000) and calculated based on Boyle's law. Gas diffusivity in soil (D_s) was measured using the one-chamber, one-gas method (Schjønning, Eden, Moldrup, & de Jonge, 2013), and D_s/D_o was calculated by relating D_s to the diffusion of O_2 in the air, D_o (0.205 cm^2 s^{-1} at 20 °C and atmospheric pressure; Smithsonian Physical Tables).

Soil samples were then divided into eight groups for measurements of PR with a micro-penetrometer at −20, −40, −60, −80, −100, −300, −500, and −1,000 hPa matric potential, for which an additional saturation and drainage process was followed. The core PR readings were made using a penetrometer probe with 1 mm basal diameter, 0.8 mm shaft diameter, and 30° cone angle. In each soil sample, three penetrations were conducted at a rate of 4 mm min^{-1} to 20 mm depth by an Instron loading frame. For each soil sample, arithmetic averages were calculated for 5–20 mm depth from all penetrations. After measuring core PR, the samples were oven-dried at 105 °C to estimate soil dry bulk density (ρ_b).

2.6 | LLWR

Data obtained from the collected 100-cm^3 soil cores were used for further calculation of the LLWR in the subsoil. The LLWR was determined using two approaches: da Silva et al. (1994) and Pulido-Moncada and Munkholm (2019). To determine the LLWR as described in da Silva et al. (1994), the variation of the water content with ρ_b was calculated at the critical limits of ε_a, FC, WP, and PR. The critical threshold of the ε_a was set at 10% (Wesseling & Van Wijk, 1957), the FC at −100 hPa matric potential, the WP at −15,000 hPa, and the PR at 2.0 MPa (Taylor, Roberson, & Parker, 1966). These critical values are commonly used for Danish soils.

The functional relationship between water content and matric potential was fitted using Equation 1 (Williams, Ross, & Bristow, 1989). The functional relationship of PR, water content, and ρ_b was determined using Equation 2 (Busscher & Sojka, 1987), and the variation with ρ_b of the water content at the limiting air-filled porosity ($\theta\varepsilon_{a,\,10\%}$) was found using Equation 3 (da Silva et al., 1994):

$$\theta = \exp(a + b\rho_b) \cdot \varphi^c \quad (1)$$

where θ is the soil volumetric water content (m^3 m^{-3}); φ is the matric potential; and a, b, and c are empirical parameters;

$$PR = d \cdot \theta^e \cdot \rho_b^f \quad (2)$$

where θ is the soil volumetric water content (m^3 m^{-3}), and d, e, and f are empirical parameters; and

$$\theta\varepsilon_{a,10\%} = \left(1 - \frac{\rho_b}{\rho_s}\right) - 0.1 \quad (3)$$

where ρ_s is the soil particle density (here assumed to be 2.65 Mg m^{-3}), and 0.1 is the limiting air-filled porosity at 10%.

According to the da Silva et al. (1994) approach, the upper limit of LLWR is defined as equal to the value of either θ_{FC} or $\theta\varepsilon_{a,10\%}$, whichever is the smaller, and the lower limit is equal to θ_{WP} or θ_{PR}, whichever is the larger.

The refinement of the LLWR proposed by Pulido-Moncada and Munkholm (2019) recalculates the upper and lower limits of the LLWR concept by using, respectively, the ε_a at which

0.005 of the D_s/D_o is reached ($\varepsilon_{a,0.005}$) and the fraction of readily available water (RAW). The refined LLWR is then defined as the water range between the $\theta\varepsilon_{a,0.005}$ and θ_{RAW}.

The refined upper limit, $\varepsilon_{a,0.005}$, estimates the variation in ε_a related to pore connectivity, and it was calculated by the power-law model as suggested by Kadžienė et al. (2011) using Equations 4 and 5.

$$D_s/D_o = \alpha \cdot \varepsilon_a^{\beta} \tag{4}$$

$$\theta\varepsilon_{a,0.005} = \left(1 - \frac{\rho_b}{\rho_s}\right) - \left(\frac{D_s/D_o}{\alpha}\right)^{1/\beta} \tag{5}$$

where α and β are empirical parameters.

The refined lower limit for LLWR, based on the RAW, expresses the boundary at which plants suffer physiological water stress (θ_{RAW}) and was calculated from the RAW concept using Equations 6, 7, and 8 (Silva et al., 2015).

$$RAW = d_{ETO} \cdot TAW \tag{6}$$

where d_{ETO} is the crop evapotranspiration depletion factor; a d_{ETO} value of 0.55 was used in this study as the average value recommended for spring barley and winter wheat because d_{ETO} varies from 0.30 to 0.70 depending on the root depth and evapotranspiration rate (Allen, Pereira, Raes, & Smith, 1998). The d_{ETO} value of the crops depends on the evaporative demands, but it was neither measured nor estimated and instead assumed a constant value throughout the growing period (Denmead & Shaw, 1962). TAW is the total soil available water, which is defined as the water content between FC and WP (Allen et al., 1998).

$$RAW = \theta_{FC} - \theta_{RAW} \tag{7}$$

Replacing in Equation 6 the RAW concept (Equation 7) and the TAW concept, then:

$$\theta_{RAW} = \theta_{FC} - \rho \cdot (\theta_{FC} - \theta_{WP}) \tag{8}$$

where θ_{FC} and θ_{WP} are the variation in water content with ρ_b, calculated by Equation 1, assuming −100 and −15,000 hPa for FC and WP, respectively.

2.7 | Water and aeration stress day

The upper and lower limits of the LLWR estimated from both the da Silva et al. (1994) and Pulido-Moncada and Munkholm (2019) approaches were used in the calculation of the water and aeration stress day (ASD) indices.

The water stress day (WSD), as proposed by Benjamin, Nielsen, and Vigil (2003), aims to capture in-season water dynamics to better determine the effects of soil condition on plant growth. The WSD is calculated as the amount of water stress the plant is subjected to during the growing season (Equation 9):

$$WSD = \theta - \theta_{LL} \tag{9}$$

where θ is the daily water content of the soil, and θ_{LL} is the lower limit of the LLWR for any day that $\theta < \theta_{LL}$; otherwise, WSD = 0.

Based on the WSD, we propose in Equation 10 a calculation of the amount of aeration stress (ASD) the plant is subjected to during the growing season:

$$ASD = \theta - \theta_{UL} \tag{10}$$

where θ is the daily water content of the soil, and θ_{UL} is the upper limit of the LLWR for any day that $\theta > \theta_{UL}$; otherwise, ASD = 0.

For comparison between years, WSD and ASD calculated for each plot were integrated over time (Equation 11) within two fixed dates covering a significant part of the growing season:

$$S_t = \Sigma_{i=1}^{n} \left\{\left[X_i + \left(X_{i+1}\right)\right]/2\right\} \cdot \left(t_{i+1} - t_i\right) \tag{11}$$

where S_t is the cumulative WSD or ASD values at time t (day), n is the number of considered time intervals i, and X is either WSD or ASD. If not measured, WSD and ASD values on 12 April and 30 June were obtained by linear interpolation.

2.8 | Vegetation index and yield

The relative vegetation index (RVI) was calculated as the ratio between the hemispherical–conical reflectance in a near-infrared band at 740–820 nm (NIR) and a photosynthetically active band at 400–700 nm (PAR) (Petersen, Jensen, & Mogensen, 2002):

$$RVI = \frac{NIR}{PAR} = \frac{NIR_r/NIR_i}{PAR_r/PAR_i} \tag{12}$$

where the suffixes r and i stand for reflected and incident fluxes, respectively.

Harvesting and weighing of grains from each plot were performed using a Haldrup plot combine harvester. Plant productivity was assessed with the yield from harvesting 90 m^2 per plot.

2.9 | Statistical analyses

A nonparametric Kruskal–Wallis test was conducted to detect statistical differences in LLWR limits and compaction treatment effects on in-season water dynamic parameters. Analysis of variance was used to determine significant differences for yield and RVI. To evaluate the association between in-season water dynamic indicators and yield and RVI, a Spearman correlation analysis was performed. A criterion of 5% was selected to represent statistical significance. All data were analyzed using the statistical package SPSS (version 24, SPSS Inc.).

3 | RESULTS AND DISCUSSION

3.1 | Climate conditions during the growing seasons

Figure 1 shows the daily precipitation, reference evapotranspiration, and mean temperatures during the growing seasons in 2017–2019. Compared with the long-term baseline of 1961–1990 (Jensen, 1996), the total monthly precipitation in 2017 was higher during the growing season for spring barley, except for May (i.e., 65 [+25], 27 [−17], 93 [+40], and 95 [+27] mm from April to July, respectively). The growing season for winter wheat in 2017–2018 was characterized by generally higher precipitation than the baseline from September to March (+72, +26, +12, +3, +21, −17, +49 mm, respectively) and lower precipitation than the baseline from April to July (−10, −21, −48, and −50 mm, respectively). In the growing season 2018–2019, precipitation was lower than the baseline from September to November (−31, −4, −34 mm) but generally higher from December to July (+25, +21, +12, +63, -26, +10, +11, −23 mm), except in April and July.

The mean monthly air temperature in 2017 was fairly similar to the baseline of 1961–1990 from April to July. For the first year of winter wheat (2017–2018), the temperature was higher than the baseline from October to January (+2.1,+1.1,+2.6, and +3.3 ˚C) and from April to July (+3.5, +4.8, +3.1, and +4.7 ˚C). In the growing season 2018–2019, temperatures were similar to the baseline in autumn but higher from December to the end of the growing season (+3, +2.2, +5, +3.7, +3.2, +0.1, +3.1, and +1.6 ˚C), except in May and July when the mean temperatures were, respectively, 4.5 and 4.7 ˚C lower than in 2018.

The cumulative monthly reference evapotranspiration was slightly lower than the long-term baseline during the period from April to July in 2017. For winter wheat 2017–2018, the low reference evapotranspiration in the autumn-winter period was similar to the baseline, except in February when it was +12.9 mm and in March when it was −3.9 mm. From April to July 2018, evapotranspiration reached higher values than the baseline (+8, +24, +23, and +36 mm, respectively). In the second growing period for winter wheat (2018–2019), the cumulative reference evapotranspiration was similar to the baseline, except from April to July (+24, −10, +18, and +9 mm, respectively). This was also a period with lower evapotranspiration than the previous growing season, except in April.

3.2 | Field PR and water content

The field PR data revealed values ≤0.5 MPa with no compaction effect in the 0.1-to-0.2-m layer ($p > .05$) (Figure 2). This was expected because plowing was conducted annually in the experimental field. A marked increment in field PR, with values ≥1.0 MPa, was evident below the plowed layer with both treatments. Traffic stress caused significantly larger field PR ($p < .05$), reaching a maximum value of 2.25 MPa at ~0.3–0.5 m depth. This is in agreement with the results found in the same experiment by Pulido-Moncada et al. (2020), which indicated that compaction significantly increased ρ_b and decreased gas transport for depths of 0.3 and 0.5 m.

The compaction treatments also significantly affected soil water content at 0.3–0.4 m depth (Figure 3) in 2017–2019. In general, larger volumetric water content was registered for the compacted subsoil compared with the control ($p < .05$) during April and May at 0.3–0.4 cm depth, whereas no significant differences were found in June at any depth.

Given that our results show no significant differences in water content of the plowed topsoil, further evaluation of water content dynamics was conducted only at 0.3 and 0.6 m depth.

3.3 | Water content variation with bulk density

Results from the present study show that θ_{FC} and θ_{PR} were the upper and lower LLWR limits, according to the da Silva et al. (1994) approach (Figure 4). After compaction, $\theta\varepsilon_{a,10\%}$ and θ_{PR} were the limiting boundaries, with a very narrow range between θ_{FC} and the $\theta\varepsilon_{a,10\%}$.

When the refined approach by Pulido-Moncada and Munkholm (2019) was calculated, the LLWR between $\theta\varepsilon_{a,0.005}$ and θ_{RAW} was also drastically reduced by compaction. However, the refined limits provided a broader range compared with the da Silva et al. (1994) approach (Figure 4). In a previous study from the same experiment, Pulido-Moncada and Munkholm (2019) also reported that, 2 yr after completion of the compaction experiment, traffic stress significantly reduced the LLWR at the measured range

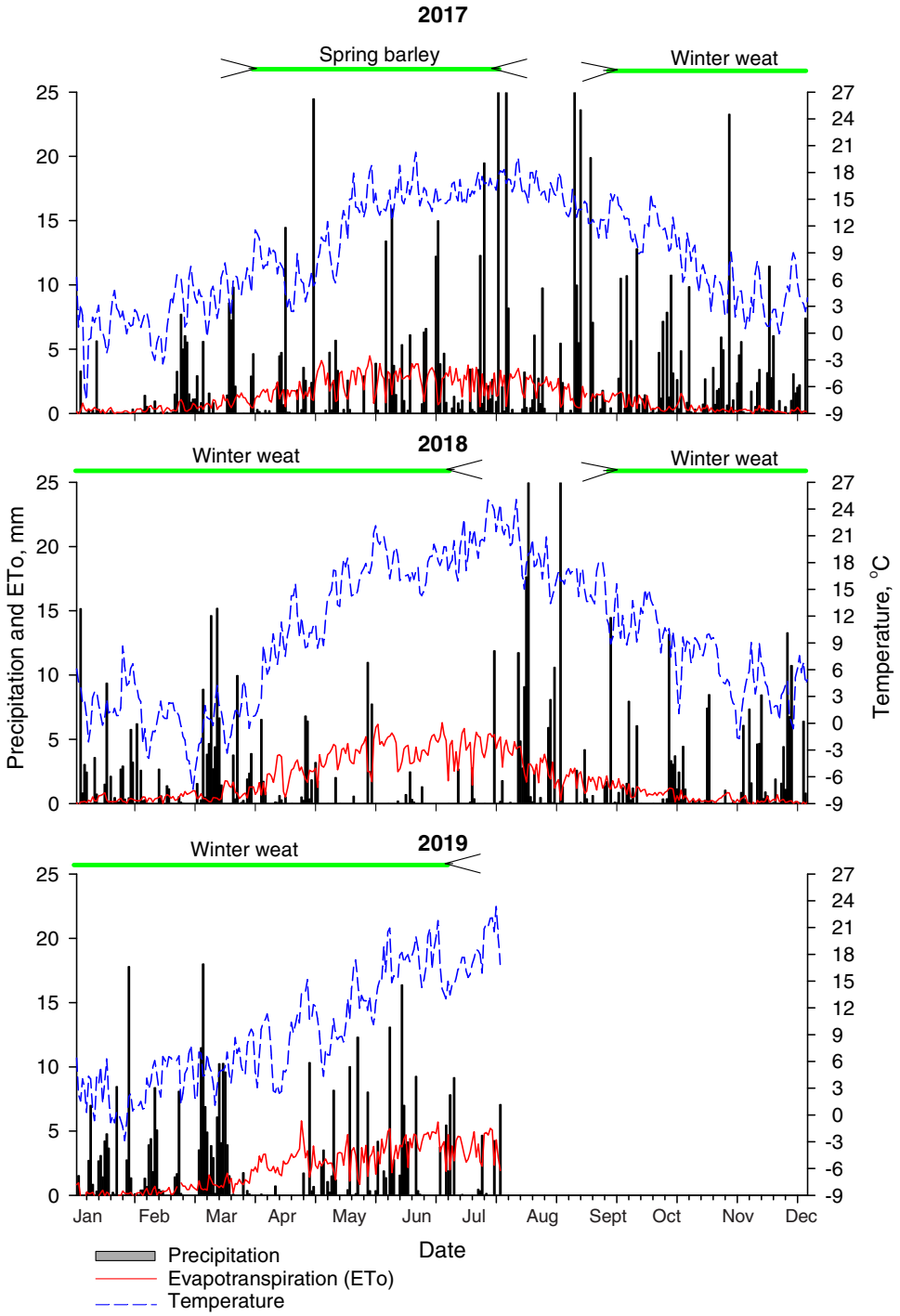

FIGURE 1 Daily precipitation, Penman reference evapotranspiration, and average air temperature at 2.0 m height during the growing season in 2017, 2018, and 2019.

in ρ_b at 0.3, 0.5, and 0.7 m depth. This was contrary to the study conducted by Benjamin et al. (2003) on a loam soil from the United States, where LLWR did not change significantly with changes in ρ_b below 0.3 m depth.

The volumetric water content for the limiting factors considered by the two LLWR approaches was estimated at the mean ρ_b for the control and compacted soil at 0.3 and 0.6 m depth (Table 2) by interpolation (Figure 4a,b). It was assumed that the water content variation with ρ_b at 0.3 m depth was applicable at 0.6 m depth because of a similar ρ_b distribution in the deeper subsoil layer. The mean ρ_b of the 0.5-m soil layer from samples taken in 2017 (Pulido-Moncada et al., 2020) was assumed to represent the conditions at 0.6 m, based on the LLWR results from 0.5 and 0.7 m depth at the same experiment assessed by Pulido-Moncada and Munkholm (2019).

TABLE 2 Mean dry bulk density and the corresponding volumetric water content for the potentially limiting factors considered by the two least limiting water range approaches under study

	Bulk density	θ_{FC}	$\theta\varepsilon_{a,10\%}$	θ_{PR}	θ_{WP}	$\theta\varepsilon_{a,0.005}$	θ_{RAW}
	Mg m^{-3}	m^3 m^{-3}					
0.3-m depth							
Control	1.62	0.28	0.29	0.28	0.21	0.33	0.24
Compacted	1.77	0.28	0.23	0.30	0.21	0.26	0.24
0.6-m depth							
Control	1.60	0.29	0.30	0.26	0.20	0.34	0.24
Compacted	1.65	0.29	0.29	0.29	0.22	0.31	0.25

Note. Mean bulk density values correspond to those reported by Pulido-Moncada et al. (2020). Volumetric water content at −100 hPa (i.e., field capacity, θ_{FC}), at 10% of air-filled porosity ($\theta\varepsilon_{a,10\%}$), at −15,000 hPa (i.e., wilting point, θ_{WP}), at 2 MPa of penetration resistance (θ_{PR}), at the air-filled porosity at which relative gas diffusivity reaches 0.005 ($\theta\varepsilon_{a,0.005}$), and at the critical moisture level based on the definition of readily available water (θ_{RAW}).

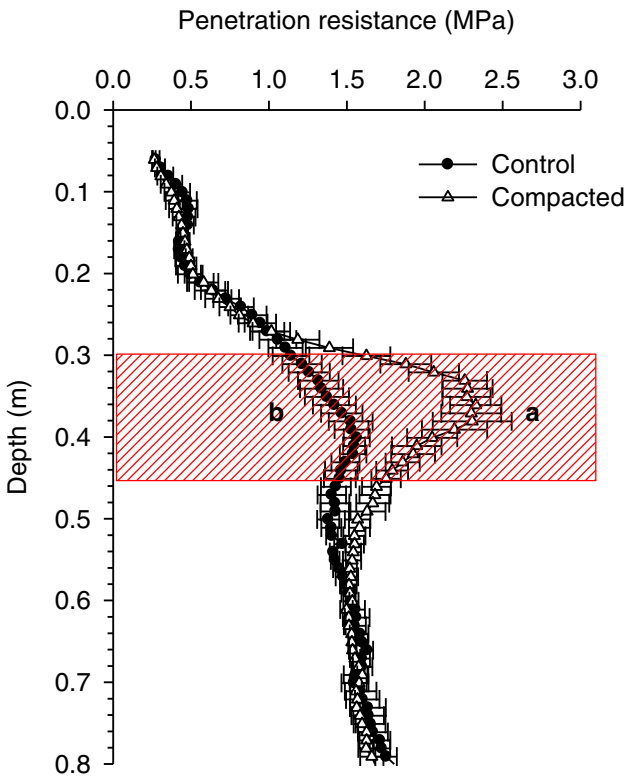

FIGURE 2 Penetration resistance measured in the field in 2017 at a soil water content near field capacity. Control soil was not experimentally trafficked, and compacted soil underwent traffic stress with a tractor–slurry trailer combination applying ~58 kN wheel load. Bars indicate SE. Different letter in the shaded area indicate significant difference between treatments for 0.05-m depth intervals ($p \leq .05$).

3.4 | In-season water content dynamics within limiting boundaries

The water content limits at the mean values of ρ_b shown in Table 2 were plotted together with measured water content in Figure 5 to identify in-season variation of stresses related to soil water content. For the control soil at 0.3 m depth, the water range displayed between the da Silva et al. (1994) limits suggests that during the 3 yr of evaluation substantial water stresses occurred during the growing seasons, reaching values equal to or lower than θ_{WP} between late April and mid-May. When considering the refined limits, the control plots at 0.3 m depth show that in 2017 water contents were lower than the dry limit during the whole measuring period but in 2018 and 2019 were lower than the dry limit only from 17 May and 24 April and onward, respectively.

In the compacted plots, at 0.3 m depth, θ_{PR} becomes larger than $\theta\varepsilon_{a,10\%}$ and θ_{FC}, indicating that mechanical soil conditions restricted root growth and thus soil water accessibility during the 3 yr. The refined limits suggest instead that the water content was within the boundaries ($\theta\varepsilon_{a,0.005} > \theta > \theta_{RAW}$) during the first 2 wk of April in 2017, during 5 d in mid-May in 2018, and at the beginning of April in 2019.

The in-season water dynamics in the control plots at 0.6 m depth show that using the da Silva et al. (1994) limits revealed a narrow period with no water content restriction from 4 May to 16 June in 2017, from 23 May to 9 June in 2018, and from 25 May to 30 June in 2019. However, the refined LLWR by Pulido-Moncada and Munkholm (2019) identified no water limitation ($\theta\varepsilon_{a,0.005} > \theta > \theta_{RAW}$) for the entire growing season, except in 2018 and 2019 when a slight water excess occurred until 12 May 2018, and until 1 May 2019.

For the compacted soil at 0.6 m, $\theta\varepsilon_{a,10\%}$, θ_{FC}, and θ_{PR} had the same value at the mean ρ_b of 1.65 Mg m^{-3}, indicating that a maximum restriction for water availability exits throughout the growing seasons. In contrast, the water range set by $\theta\varepsilon_{a,0.005}$ and θ_{RAW} suggests that slight water excess occurred until late April in 2017 and until late May in 2018 and 2019. It is important to highlight that, at 0.6 m depth, the water content was always above θ_{RAW} in the control and the compacted soil (except from 1 June 2018), which indicates that during dry periods roots reaching deeper into the subsoil had access to available water.

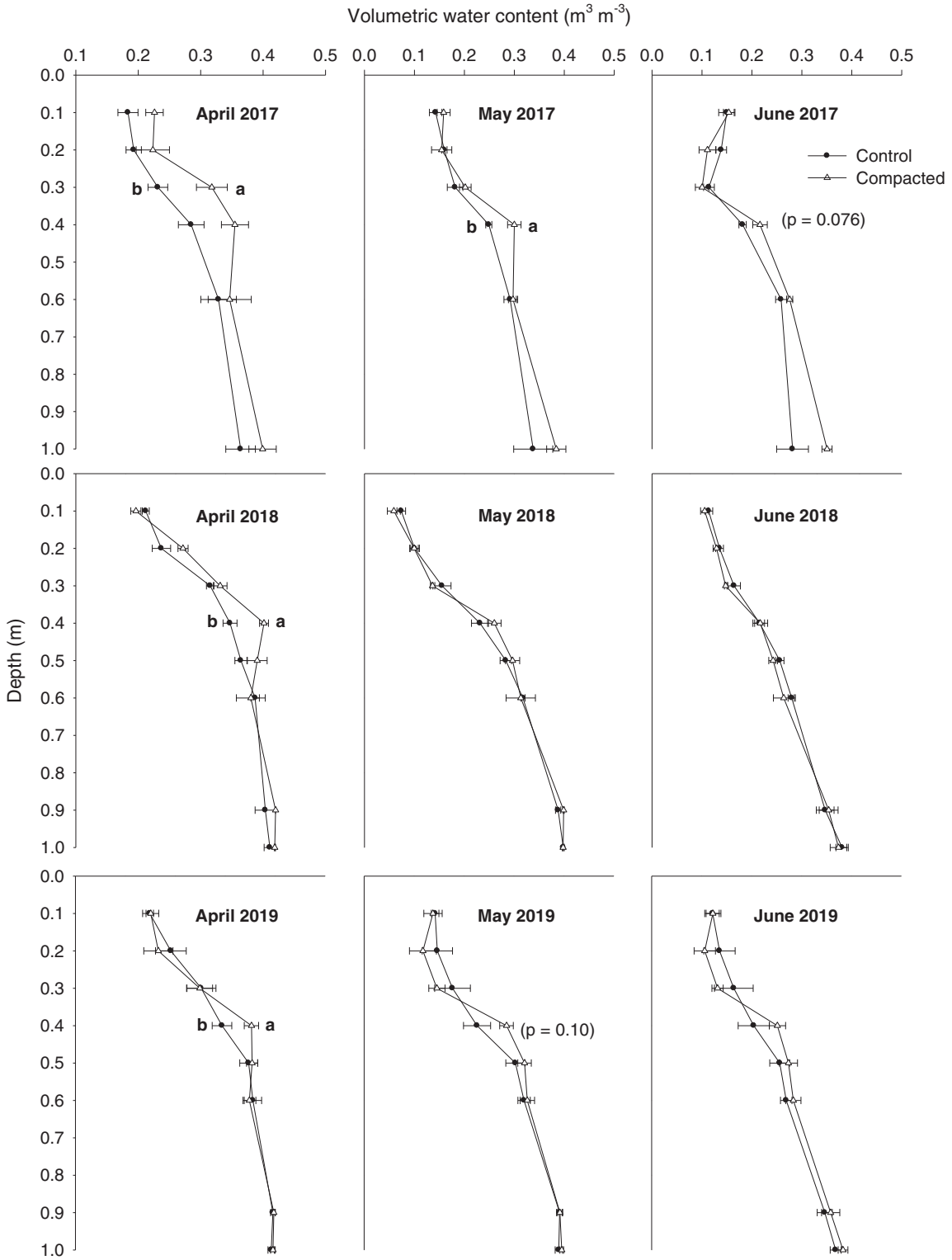

FIGURE 3 Soil water content measured with a multisensor capacitance PR2 Profile Probe down to 1.0 m soil depth at different dates from 2017 to 2019. Bars indicate SE. Values followed by different letters are significantly different between treatments for the same depth ($p \leq .05$). Spring barley was sown in 2017 and winter wheat cultivar Sheriff in 2018 and 2019.

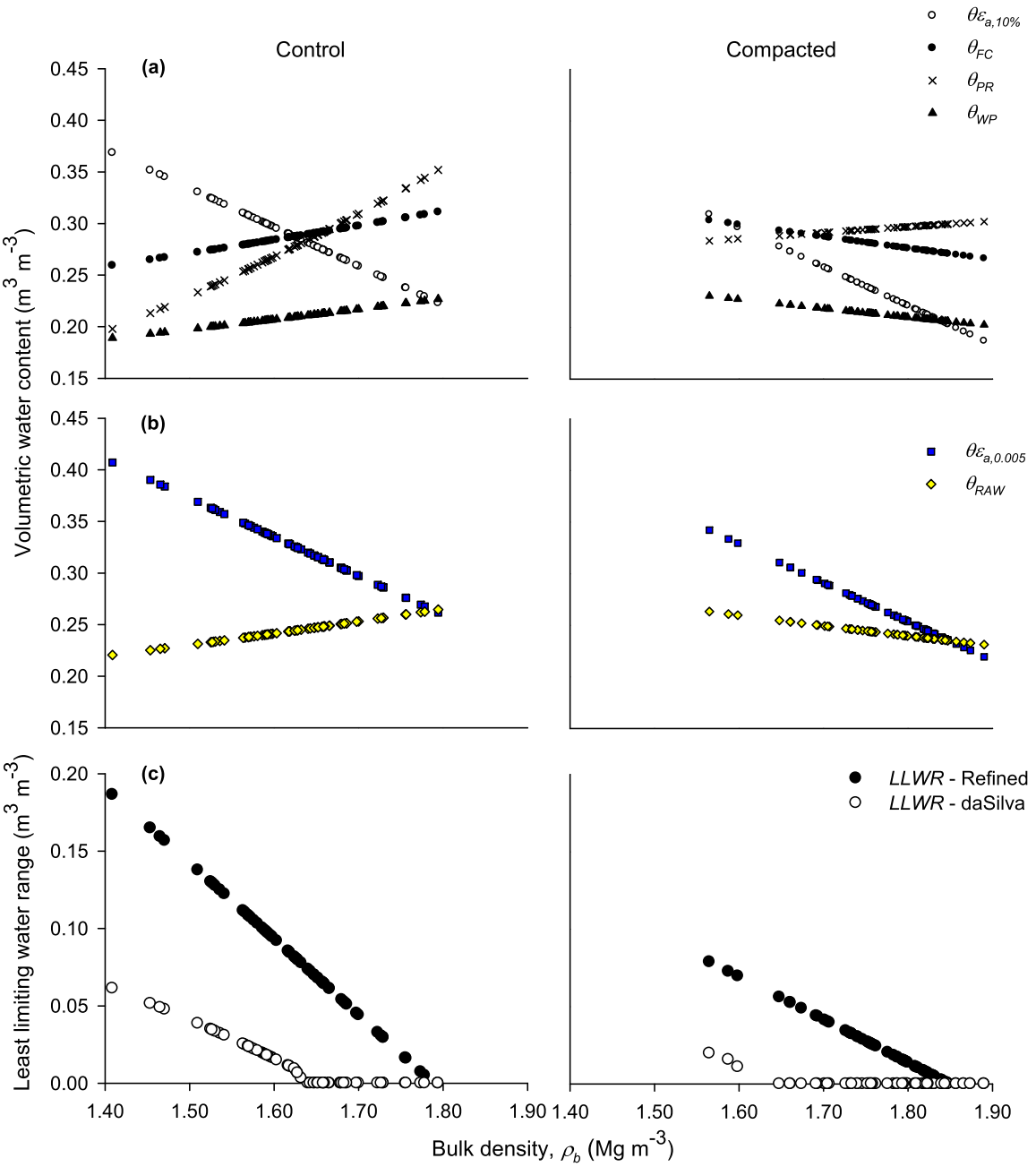

FIGURE 4 (a) The da Silva et al. (1994) approach integrates the volumetric water content variation with soil bulk density at −100 hPa (i.e., field capacity, θ_{FC}), at 10% of air-filled porosity ($\theta\varepsilon_{a,10\%}$), at −15,000 hPa (i.e., wilting point, θ_{WP}) and at 2 MPa of penetration resistance (θ_{PR}). (b) The refined approach proposed by Pulido-Moncada and Munkholm (2019) considers the air-filled porosity at which relative gas diffusivity reaches 0.005 ($\theta\varepsilon_{a,0.005}$) as the upper limit and the critical moisture level based on the definition of readily available water (θ_{RAW}) as the lower limit. (c) The resulting least limiting water range (LLWR) in the light of the two approaches for Taastrup site at 0.3 m depth.

3.5 | In-season WSD and ASD dynamics

In general, the results from the estimation of the ASD and WSD showed that greater ASD and smaller (numerically greater) WSD was estimated when using the da Silva et al. (1994) than the Pulido and Munkholm (2019) LLWR approach at any combination of treatment and depth ($p < .05$) (Supplemental Figures S1 and S2). We used the Pulido-Moncada and Munkholm (2019) LLWR approach for further analysis of the in-season water dynamics because the da Silva et al. (1994) approach suggested that at mean ρ_b there was zero or very small LLWR for root development and growth (Figures 4 and 5).

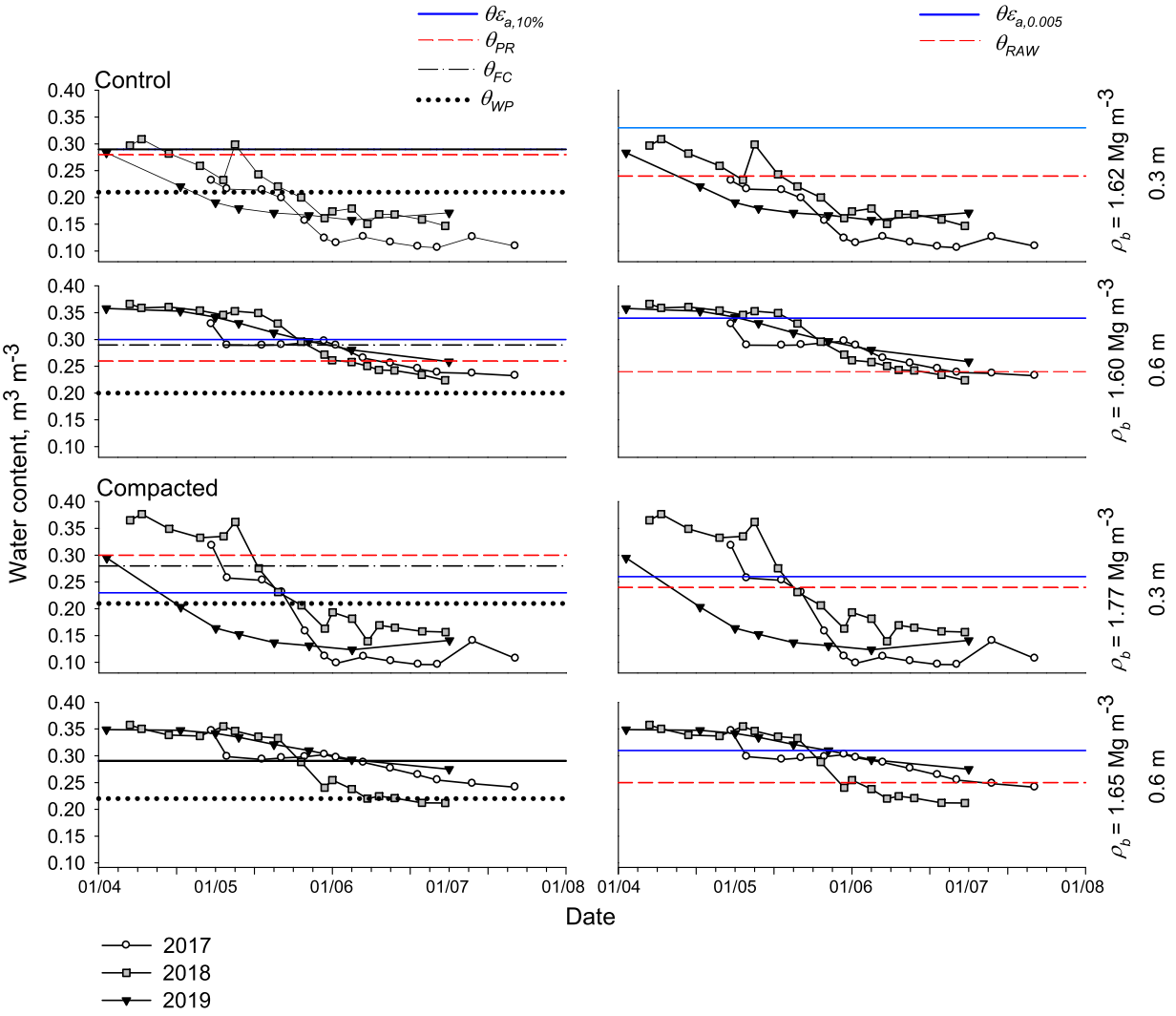

FIGURE 5 Average soil water content ($m^3\ m^{-3}$) at 0.3 and 0.6 m depth measured from April to July in 2017, 2018, and 2019. The horizontal lines represent the upper and lower limits of the least limiting water range (LLWR) at the mean bulk density value of each treatment × depth combination. The da Silva et al. (1994) approach (left panel) integrates the water contents at −100 hPa (i.e., field capacity, θ_{FC}), at 10% of air-filled porosity ($\theta\varepsilon_{a,10\%}$), at −15,000 hPa (i.e., wilting point, θ_{WP}), and at 2 MPa of penetration resistance (θ_{PR}). The refined approach (right panel) proposed by Pulido-Moncada and Munkholm (2019) considers the air-filled porosity at which relative gas diffusivity reaches 0.005 ($\theta\varepsilon_{a,0.005}$) and the critical moisture level based on the definition of readily available water (θ_{RAW}).

When the refined limits were considered, an overall higher estimation of cumulative ASD was obtained for the compacted soil than for the control at 0.3 m depth ($p < .05$), except in 2019 (Table 3). No significant compaction effect on the cumulative ASD was found at 0.6 m depth in the 3 yr of study. The cumulative WSD during the growing period was not significantly affected by compaction within each year of evaluation at any depth ($p > .05$).

When winter wheat growing years were considered together, the compaction effect on cumulative ASD was strongly significant at 0.3 m depth ($p < .01$), but no effect was found at 0.6 m depth ($p > .05$).

3.6 | LLWR/weather factors ruling the grain yield and maximum RVI

The LLWR results indicating impeded root growth conditions for compacted soil compared with the control are not reflected in reduced crop yield, with no significant compaction effect on grain yield or maximum RVI ($p > .05$) (Table 4). This is contradictory to the reduction in yield and the inhibition effect on root development by subsoil compaction that has been widely reported elsewhere (Oussible, Crookston, & Larson, 1992; Qin et al., 2018; Schneider & Don, 2019; Taylor & Brar, 1991). The lack of subsoil compaction effect on yield in

TABLE 3 Cumulative aeration stress day (Cum. ASD) and water stress day (Cum. WSD) indicators, calculated for the period 12 April to 30 June using Equation 11

Year	Crop	Depth (m)	Treatment	Cum. ASD	Cum. WSD
2017	spring barley	0.3	control	0.0b	−5.2a
			compacted	0.2a	−4.9a
		0.6	control	0.0a	−0.1a
			compacted	0.1a	0.0a
2018	winter wheat	0.3	control	0.1b	−2.5a
			compacted	3.1a	−2.9a
		0.6	control	0.5a	−0.1a
			compacted	1.7a	−0.7a
2019	winter wheat	0.3	control	0.0a	−6.4a
			compacted	0.7a	−7.7a
		0.6	control	0.9a	−0.0a
			compacted	2.2a	−0.0a
p Value					
Compaction effect within years 2018–2019		0.3		.021	.753
		0.6		.247	.666
Year effect between 2018 and 2019		0.3		.100	.016
		0.6		.343	.015

Note. Values are based on the refined limits of the least limiting water range. Values in a column followed by the same letter are not significantly different between treatments for the same depth and year ($p \geq .05$).

TABLE 4 Means of the grain yield and the maximum value of the relative vegetation index (max_RVI) for the three years under study

Year	Crop	Treatment	Yield (kg ha^{-1})	max_RVI
2017	spring barley	control	7,554a	13.5a
		compacted	7,774a	13.4a
2018	winter wheat	control	7,038a	8.0a
		compacted	6,782a	8.3a
2019	winter wheat	control	9,142a	15.5a
		compacted	9,543a	16.0a
p Value				
Compaction effect within years 2018–2019			.927	.914
Year effect between 2018 and 2019			<.001	<.001

Note. Values in a column followed by the same letter are not significantly different between treatments in the same year ($p \geq .05$).

our study may be associated with the fact that the studied subsoil was initially already compacted and went to a more severe compaction state after heavy traffic experimentation. For control soil, maximum PR values of 1.3, 1.2, and 1.6 MPa at 0.3, 0.5, and 0.8 m depth, respectively, were reported by Schjønning et al. (2016).

Additionally, Håkansson and Reeder (1994), summarizing a series of studies, found that topsoil compaction caused the major part of the crop response in the first year after compaction and that the effect disappears after 2 yr. Subsoil compaction also responsible for part of the crop response appears to be constant, and the effect disappears after 5–10 yr. This compaction persistency/crop response model was cited to be highly dependent on soil clay content. In a previous study, Schjønning et al. (2016) showed that yield decline was mainly associated to topsoil compaction during the annual heavy traffic trial in three sandy loam fields (including the studied field). Our results may hence suggest that subsoil compaction does

TABLE 5 Spearman's rho coefficients between grain yield, maximum value of the relative vegetation index (max_RVI), cumulative aeration stress day (cum. ASD), and cumulative water stress day (cum. WSD) in 2018–2019

	Grain yield	max_RVI
	1.000	.903**
0.3 m depth		
Cum. ASD	−.547*	−.408
Cum. WSD	−.744**	−.671**
0.6 m depth		
Cum. ASD	.286	.416
Cum. WSD	.208	.447

*Significant at the .05 probability level.
**Significant at the .01 probability level.

not have a strong residual effect 4 yr after termination of the compaction experimentation on the temperate sandy loam soil under study.

For spring barley, the yield obtained in 2017 was 25% larger than the previous 10-yr average for the region according to Statistics Denmark (https://www.statistikbanken.dk/statbank5a/selectvarval). Although spring barley is sensitive to wet conditions during seedling emergence (Peltonen-Sainio et al., 2010), in Taastrup a wet pre-seeding period (February–March) and the wet April (65 mm) in 2017 (Figure 1) appear not to have caused a yield reduction. The deficit of water, estimated in the remaining growing season in 2017, for both control and compacted soil at 0.3 m depth, was likely not of significance because there was available water deeper in the soil profile, as shown by the 0.6-m results. Additionally, similar temperatures to normal years and low or normal evaporative demand characterized the growing season for spring barley. Hence, favorable conditions, both aboveground and belowground, were present for spring barley in 2017.

In 2018, the average grain yield for winter wheat was 6,910 kg ha^{-1}, which was lower than the 10-yr average of 8,141 kg ha^{-1} on the island of Zealand (Statistics Denmark -https://www.statistikbanken.dk/statbank5a/selectvarval). On the other hand, in 2019, the winter wheat grain yield was 1,202 kg ha^{-1} higher than the 10-yr average. Thus, the 2018 yield was 26% lower than the 2019 yield ($p < .001$) (Table 4). The maximum RVI for winter wheat was also significantly lower in 2018 compared with 2019 ($p < .001$) (Table 4). The maximum RVI in 2018 (reached mid-May) was on average 8.2, which is very small compared with 13–15 in a normal year (Petersen et al., 2002). An RVI of 8.2 can be translated into a leaf area index of ~1.7, which is not enough to obtain full ground cover and thus explains the low grain yield. This is supported by the significant correlation found between maximum RVI and grain yield ($r = .90$; $p < .001$) for winter wheat within the period 2018–2019 (Table 5).

The in-season soil water dynamic indicators estimated for the period between April and July in 2018–2019 at 0.3 m depth was partially correlated to grain yield. The cumulative ASD and WSD indicators were both negatively correlated with grain yield ($r = -.547$; $p < .05$ and $r = -.744$; $p < .01$, respectively) (Table 5). The inversely proportional relation found between WSD (negative numeric values) and grain yield indicates that the lack of water at 0.3 m depth was important for crop productivity because roots reached deeper layers with available water content.

In 2018, the loss in grain yield and maximum RVI, compared with 2019, appear to have been caused mainly in the spring. The weather went from a very cold March to a hot and dry period in April, May, and June (Figure 1). No root growth was evaluated, but root development in April 2018 was most likely poor due to late sowing and a wet autumn/winter (shallow water table) with total precipitation of 498.3 mm from September 2017 to March 2018. The tillering stage with three shoots (23 on the BBCH scale) was reached on 12 Apr. 2018 and on 2 Apr. 2019 (data not shown). Few tillers after the winter and a very short time for further tillering in spring 2018 strongly indicate poor early root development in 2018 compared with 2019. The low RVI peak in late May 2018, despite expected poor early-season root growth, could not alone be explained by an excess of soil water (ASD) in April and the beginning of May (Supplemental Figure S1) because similar cumulative ASD was found for both years 2018 and 2019 at 0.3 and 0.6 m depth (Table 3).

In April 2018, the mean air temperature reached 9 ˚C after a mean of 0.2 ˚C in March and increased to 15.5 ˚C in May and 17.6 ˚C in June. Because the optimum air temperature for grain yield is 15 ˚C (Chowdhury & Wardlaw, 1978), it is important to note that in May and June 2018 maximum air temperatures of 25–27 ˚C were registered for short periods (3–6 d). Winter wheat yield is commonly cited to be negatively affected when temperatures are >30 ˚C (Alghabari et al., 2014; Mäkinen et al., 2018). However, Peltonen-Sainio et al. (2010) found under Finnish conditions that grain yield of winter wheat is sensitive to an increase in temperature prior to and during heading, reaching up to 186 kg ha^{-1} in yield

decline per 1 °C increase in phase mean temperature. Likewise, Teixeira, Fischer, Van Velthuizen, Walter, and Ewert (2013) highlighted that when the temperature rises above 25–35 °C during the grain filling of wheat, this period will be shorter and result in a yield decrease. For wheat, a high temperature affects grain yield even at relatively high soil water contents, and when the interaction of both temperature and water stresses occurs, higher yield depletion is expected (Shah & Paulsen, 2003).

In our study, the Penman reference evapotranspiration in May (on average 3.9 mm d^{-1}) and June (4.2 mm d^{-1}) in 2018 reached values higher than the normal values for potential evaporation in Taastrup in these months (i.e., 3.0 and 3.5 mm d^{-1}, respectively). It is likely that poor (early) root development, as well as high evaporative demands (affecting all treatments), might have worsened water stress late in the season. As mentioned above, in late May 2018 water content reached values close to or lower than θ_{RAW} at both depths and even reached below θ_{WP} at 0.3 m, increasing the WSD rapidly at that time (Supplemental Figure S2). Comparison between 2018 and 2019 showed that at 0.3 m depth numerically less cumulative WSD occurred in 2018 compared with 2019 ($p = .016$) (Table 3) because dry conditions started earlier in mid-April in 2019 (Figure 3). However, at 0.6 m higher cumulative WSD occurred in 2018 compared with 2019 ($p = .015$) (Table 3) because markedly drier conditions at depth were recorded from late May in 2018 (Figure 3). Curled leaves were observed in June after anthesis, which is a well-known symptom of drought stress caused by high temperatures and, therefore, evaporative demands as well as UV radiation (Kadioglu, Terzi, Saruhan, & Saglam, 2012). Hence, during the growing season in 2018, the combination of the abovementioned factors (poor early root development [aeration stress-related], high temperatures and evaporative demands, and moderate soil water deficits during and after anthesis) is expected to have influenced rapid crop development, physiological responses (stomata closure), and yield decrease (Denmead & Shaw, 1962).

In 2019, the high grain yield and RVI obtained from both the control and compacted soil indicated crop growth were apparently not limited by water content below the dry limit at 0.3 cm depth from mid-April to end of the growing season. We expect that the plants have benefited from a better-developed root system during a drier autumn/winter of 283 mm compared with 411 mm in 2018 (Figure 1), which ensured access to water in deeper soil layers (with wider LLWR) during later stages of plant development. The 2019 winter wheat also benefitted from a lower average air temperature (10.8 °C) and reference evapotranspiration (2.7 mm d^{-1}) in May during heading compared with 2018.

Additionally, the WSD and ASD calculated from the Pulido-Moncada and Munkholm (2019) refined limits were useful indicators for evaluating the influence of in-season water dynamics on crop response in our study. Benjamin et al. (2003) found a strong positive correlation between corn yield and WSD (calculated from PR as lower limit) than with ρ_b or LLWR. The authors suggested that in-season water dynamics estimated by WSD play a large role in the determination of corn yield in their region of study with higher evaporative demands. Our results showed an opposite correlation between WSD and grain yield compared with Benjamin et al. (2003); however, it reflected some specific conditions for tile-drained soils in a northern Europe area with a severely compacted subsoil. Dry conditions in the topsoil without structural limitation force the crop to reach deeper layers for water uptake. Therefore, for the studied tile-drained soil, taking account of both aboveground and belowground factors seems to be of importance for a comprehensive evaluation of crop response. Further evaluation of the capability and applicability of the WSD and ASD indicators should be conducted for other soils, climates, and crops.

4 | CONCLUSION

Subsoil compaction increased the field PR below the plow layer, causing unfavorable conditions with an excess of water in April and beginning of May in the years when precipitation continuously exceeded the normal values in the studied area. The water content of the studied compacted subsoil falls outside the LLWR proposed by da Silva et al. (1994) during the whole growing season in most cases. The refined LLWR by Pulido-Moncada and Munkholm (2019) provides a broader range of water contents with minimum physical limitations to root growth. Compaction narrowed the LLWR at both depths; however, no significant effects of compaction on grain yield were observed. Water deficit at 0.3 m might have been compensated by roots reaching the deeper soil layer with less limiting conditions. The use of WSD and the proposed ASD as potential indicators of in-season stresses for crop growth provided knowledge of the water dynamics and the periods under stress during the growing season. Compaction significantly increased ASD in two out of three years. However, in-season water content dynamics results alone could not explain what happened aboveground in terms of grain yield. Early crop growth and development were very poor in spring of 2018. Later in the season, crop growth and development might have been governed by high temperatures and evaporative demands together with soil water deficit. Our study highlights the need to investigate more deeply the effects of subsoil compaction on in-season stresses (aboveground and belowground) affecting crop yield, such as for different crops and different soil and climatic conditions and with measurements on both soil water content and root growth dynamics.

ACKNOWLEDGMENTS

Sampling was conducted with the help of Stig T. Rasmussen and Michael Koppelgaard. Laboratory measurements were performed with the help of Bodil B. Christensen and Jørgen M. Nielsen. This paper was funded by the Ministry of Environment and Food of Denmark via the COMMIT project (GUDP Grant 34009-16-1086). The authors are also grateful to the anonymous referees for their helpful comments and suggestions.

CONFLICT OF INTEREST

The authors declare no conflict of interest.

ORCID

Mansonia Pulido-Moncada https://orcid.org/0000-0002-8920-8160

Lars J. Munkholm https://orcid.org/0000-0002-4506-9488

REFERENCES

Alakukku, L. (1996). Persistence of soil compaction due to high axle load traffic: II. Long-term effects on the properties of fine-textured and organic soils. *Soil and Tillage Research*, *37*, 223–238.https://doi.org/10.1016/0167-1987(96)01017-3

Alghabari, F., Lukac, M., Jones, H., & Gooding, M. (2014). Effect of R ht alleles on the tolerance of wheat grain set to high temperature and drought stress during booting and anthesis. *Journal of Agronomy and Crop Science*, *200*, 36–45.https://doi.org/10.1111/jac.12038

Allen, R. G., Pereira, L. S., Raes, D., & Smith, M. (1998). *FAO Irrigation and drainage paper no. 56*. Rome: FAO.

Ball, B., Batey, T., Munkholm, L. J., Guimarães, R., Boizard, H., McKenzie, D., … Hargreaves, P. (2015). The numeric visual evaluation of subsoil structure (SubVESS) under agricultural production. *Soil and Tillage Research*, *148*, 85–96.https://doi.org/10.1016/j.still.2014.12.005

Bengough, A. G., Bransby, M. F., Hans, J., McKenna, S. J., Roberts, T. J., & Valentine, T. A. (2006). Root responses to soil physical conditions; growth dynamics from field to cell. *Journal of Experimental Botany*, *57*, 437–447.https://doi.org/10.1093/jxb/erj003

Bengough, A. G., & Mullins, C. E. (1990). Mechanical impedance to root growth: A review of experimental techniques and root growth responses. *European Journal of Soil Science*, *41*, 341–358.https://doi.org/10.1111/j.1365-2389.1990.tb00070.x

Benjamin, J., Nielsen, D., & Vigil, M. (2003). Quantifying effects of soil conditions on plant growth and crop production. *Geoderma*, *116*, 137–148.https://doi.org/10.1016/S0016-7061(03)00098-3

Berisso, F. E., Schjønning, P., Keller, T., Lamandé, M., Etana, A., de Jonge, L. W., … Forkman, J. (2012). Persistent effects of subsoil compaction on pore size distribution and gas transport in a loamy soil. *Soil and Tillage Research*, *122*, 42–51.https://doi.org/10.1016/j.still.2012.02.005

Betz, C., Allmaras, R., Copeland, S., & Randall, G. (1998). Least limiting water range: Traffic and long-term tillage influences in a Webster soil. *Soil Science Society of America Journal*, *62*, 1384–1393.https://doi.org/10.2136/sssaj1998.03615995006200050034x

Beutler, A. N., Centurion, J. F., & Silva, A. P.d. (2005). Soil resistance to penetration and least limiting water range for soybean yield in a haplustox from Brazil. *Brazilian Archives of Biology and Technology*, *48*, 863–871.https://doi.org/10.1590/S1516-89132005000800002

Beutler, A. N., Centurion, J. F., Silva, A. P.d., Centurion, M. A. P.d.C., Leonel, C. L., & Freddi, O.d.S. (2008). Soil compaction by machine traffic and least limiting water range related to soybean yield. *Pesquisa Agropecuária Brasileira*, *43*, 1591–1600.https://doi.org/10.1590/S0100-204X2008001100019

Busscher, W., & Sojka, R. (1987). Enhancement of subsoiling effect on soil strength by conservation tillage. *Transactions of the ASAE*, *30*, 888–0892.https://doi.org/10.13031/2013.30493

Calonego, J. C., & Rosolem, C. A. (2011). Least limiting water range in soil under crop rotations and chiseling. *Revista Brasileira de Ciência do Solo*, *35*, 759–771.https://doi.org/10.1590/S0100-06832011000300012

Chen, G., Weil, R. R., & Hill, R. L. (2014). Effects of compaction and cover crops on soil least limiting water range and air permeability. *Soil and Tillage Research*, *136*, 61–69.https://doi.org/10.1016/j.still.2013.09.004

Chowdhury, S., & Wardlaw, I. (1978). The effect of temperature on kernel development in cereals. *Australian Journal of Agricultural Research*, *29*, 205–223.https://doi.org/10.1071/AR9780205

da Silva, A., Kay, B., & Perfect, E. (1994). Characterization of the least limiting water range of soils. *Soil Science Society of America Journal 58*, 1775–1781.https://doi.org/10.2136/sssaj1994.03615995005800060028x

da Silva, A. P., & Kay, B. (1996). The sensitivity of shoot growth of corn to the least limiting water range of soils. *Plant and Soil*, *184*, 323–329.https://doi.org/10.1007/BF00010461

Denmead, O. T., & Shaw, R. H. (1962). Availability of soil water to plants as affected by soil moisture content and meteorological conditions 1. *Agronomy Journal*, *54*, 385–390.https://doi.org/10.2134/agronj1962.00021962005400050005x

Fidalski, J., Tormena, C. A., & Silva, Á. P.d. (2010). Least limiting water range and physical quality of soil under groundcover management systems in citrus. *Scientia Agricola*, *67*, 448–453.https://doi.org/10.1590/S0103-90162010000400012

Flint, L. E., & Flint, A. L. (2002). Porosity. *Methods of Soil Analysis: Part*, *4*, 241–254.

Gonçalves, W. G., Severiano, E.d.C., Silva, F. G., Costa, K. A.d.P., Guimarães-Junnyor, W.d.S., & Melo, G. B. (2014). Least limiting water range in assessing compaction in a Brazilian Cerrado latosol growing sugarcane. *Revista Brasileira de Ciência do Solo*, *38*, 432–443.https://doi.org/10.1590/S0100-06832014000200008

Håkansson, I., & Reeder, R. C. (1994). Subsoil compaction by vehicles with high axle load: Extent, persistence and crop response. *Soil and Tillage Research*, *29*, 277–304.https://doi.org/10.1016/0167-1987(94)90065-5

Jensen, S. E. (1996). *Agroclimate at taastrup 1961–1990*. Copenhagen: Jordbrugsforlaget.

Kadioglu, A., Terzi, R., Saruhan, N., & Saglam, A. (2012). Current advances in the investigation of leaf rolling caused by biotic and abiotic stress factors. *Plant Science*, *182*, 42–48.https://doi.org/10.1016/j.plantsci.2011.01.013

Kadžienė, G., Munkholm, L. J., & Mutegi, J. K. (2011). Root growth conditions in the topsoil as affected by tillage intensity. *Geoderma*, *166*, 66–73.https://doi.org/10.1016/j.geoderma.2011.07.013

Kahlon, M. S., & Chawla, K. (2017). Effect of tillage practices on least limiting water range in Northwest India. *International Agrophysics*, *31*, 183–194.https://doi.org/10.1515/intag-2016-0051

Klein, V. A., & Camara, R. K. (2007). Soybean grain yield and least limiting water range in an oxisol under chiseled no-tillage. *Revista Brasileira de Ciência do Solo*, *31*, 221–227.https://doi.org/10.1590/S0100-06832007000200004

Lapen, D., Topp, G., Gregorich, E., & Curnoe, W. (2004). Least limiting water range indicators of soil quality and corn production, eastern Ontario, Canada. *Soil and Tillage Research*, *78*, 151–170.https://doi.org/10.1016/j.still.2004.02.004

Letey, J. (1958). Relationship between soil physical properties and crop production. In B. A. Stewart (Ed.), *Advances in soil science* (pp. 277–294). New York: Springer-Verlag.

Lynch, J. P., & Wojciechowski, T. (2015). Opportunities and challenges in the subsoil: Pathways to deeper rooted crops. *Journal of Experimental Botany*, *66*, 2199–2210.https://doi.org/10.1093/jxb/eru508

Mäkinen, H., Kaseva, J., Trnka, M., Balek, J., Kersebaum, K., Nendel, C., … Ferrise, R. (2018). Sensitivity of European wheat to extreme weather. *Field Crops Research*, *222*, 209–217.https://doi.org/10.1016/j.fcr.2017.11.008

Mohammadi, M. H., Asadzadeh, F., & Vanclooster, M. (2010). Refining and unifying the upper limits of the least limiting water range using soil and plant properties. *Plant and Soil*, *334*, 221–234.https://doi.org/10.1007/s11104-010-0377-3

Møller, A. B., Beucher, A., Iversen, B. V., & Greve, M. H. (2018). Predicting artificially drained areas by means of a selective model ensemble. *Geoderma*, *320*, 30–42.https://doi.org/10.1016/j.geoderma.2018.01.018

Olesen, S. E. (2009). Kortlægning af potentielt dræningsbehov på landbrugsarealer opdelt efter landskabselement, geologi, jordklasse, geologisk region samt høj/lavbund. In *DJF Inter Rapport Markbrug*. Aarhus, Denmark: Aarhus Universitet.

Olsen, H. (1988). Technology showcase electronic penetrometer for field tests. *Journal of Terramechanics*, *25*, 287–293.https://doi.org/10.1016/0022-4898(88)90042-0

Oussible, M., Crookston, R., & Larson, W. (1992). Subsurface compaction reduces the root and shoot growth and grain yield of wheat. *Agronomy Journal*, *84*, 34–38.https://doi.org/10.2134/agronj1992.00021962008400010008x

Peltonen-Sainio, P., Jauhiainen, L., Trnka, M., Olesen, J. E., Calanca, P., Eckersten, H., … Kozyra, J. (2010). Coincidence of variation in yield and climate in Europe. *Agriculture, Ecosystems & Environment*, *139*, 483–489.

Penman, H. L. (1948). Natural evaporation from open water, bare soil and grass. *Proceedings of the Royal Society of London A*, *193*, 120–145.

Petersen, C. T., Jensen, C. R., & Mogensen, V. O. (2002). Analysis of variation of spectral vegetation index measured in differently fertilized field barley. *Communications in Soil Science and Plant Analysis*, *33*, 1485–1506.https://doi.org/10.1081/CSS-120004296

Pulido-Moncada, M., & Munkholm, L. J. (2019). Limiting water range: A case study for compacted subsoils. *Soil Science Society of America Journal*, *83*, 982–992.https://doi.org/10.2136/sssaj2019.01.0023

Pulido-Moncada, M., Schjønning, P., Labouriau, R., & Munkholm, L. J. (2020). Residual effects of compaction on the subsoil pore system: A functional perspective. *Soil Science Society of America Journal*, *84*, 717–730.https://doi.org/10.1002/saj2.20061

Qin, R., Noulas, C., & Herrera, J. M. (2018). Morphology and distribution of wheat and maize roots as affected by tillage systems and soil physical parameters in temperate climates: An overview. *Archives of Agronomy and Soil Science*, *64*, 747–762.https://doi.org/10.1080/03650340.2017.1406078

Reichert, J., da Silva, V., & Reinert, D. (2004). Soil moisture, penetration resistance, and least limiting water range for three soil management systems and black beans yield. Presented at the 13th International Soil Conservation Organisation Conference, Brisbane.

Rüegg, K. (2000). Development, test and use of an air-pycnometer to measure air-filled porosity on undisturbed soil samples (Master's thesis). Aalborg University, Aalborg, Denmark.

Sato, M. K., Lima, H. V.d., Ferreira, R. L.d.C., Rodrigues, S., & Silva, Á. P.d. (2017). Least limiting water range for oil palm production in Amazon region, Brazil. *Scientia Agricola*, *74*, 148–156.https://doi.org/10.1590/1678-992x-2015-0408

Schjønning, P., Eden, M., Moldrup, P., & de Jonge, L. W. (2013). Two-chamber, two-gas and one-chamber, one-gas methods for measuring the soil-gas diffusion coefficient: Validation and inter-calibration. *Soil Science Society of America Journal*, *77*, 729–740.https://doi.org/10.2136/sssaj2012.0379

Schjønning, P., Lamandé, M., Crétin, V., & Nielsen, J. A. (2017). Upper subsoil pore characteristics and functions as affected by field traffic and freeze–thaw and dry–wet treatments. *Soil Research*, *55*, 234–244.https://doi.org/10.1071/SR16149

Schjønning, P., Lamandé, M., Munkholm, L. J., Lyngvig, H. S., & Nielsen, J. A. (2016). Soil precompression stress, penetration resistance and crop yields in relation to differently-trafficked, temperate-region sandy loam soils. *Soil and Tillage Research*, *163*, 298–308.https://doi.org/10.1016/j.still.2016.07.003

Schneider, F., & Don, A. (2019). Root-restricting layers in German agricultural soils. Part I: Extent and cause. *Plant and Soil*, *442*, 433–451.https://doi.org/10.1007/s11104-019-04185-9

Shah, N., & Paulsen, G. (2003). Interaction of drought and high temperature on photosynthesis and grain-filling of wheat. *Plant and Soil*, *257*, 219–226.https://doi.org/10.1023/A:1026237816578

Silva, B. M., Oliveira, G. C., Serafim, M. E., Silva, É. A., Ferreira, M. M., Norton, L. D., & Curi, N. (2015). Critical soil moisture range for a coffee crop in an oxidic Latosol as affected by soil management. *Soil and Tillage Research*, *154*, 103–113.https://doi.org/10.1016/j.still.2015.06.013

Silva, B. M., Oliveira, G. C., Serafim, M. E., Silva, É. A., Guimarães, P. T. G., Melo, L. B. B., … Curi, N. (2019). Soil moisture associated with least limiting water range, leaf water potential, initial growth and yield of coffee as affected by soil management system. *Soil and Tillage Research*, *189*, 36–43.https://doi.org/10.1016/j.still.2018.12.016

Taylor, H., & Brar, G. (1991). Effect of soil compaction on root development. *Soil and Tillage Research*, *19*, 111–119.https://doi.org/10.1016/0167-1987(91)90080-H

Taylor, H. M., Roberson, G. M., & Parker, Jr., J. J. (1966). Soil strength-root penetration relations for medium-to coarse-textured soil materials. *Soil Science*, *102*, 18–22. https://doi.org/10.1097/00010694-196607000-00002

Teixeira, E. I., Fischer, G., Van Velthuizen, H., Walter, C., & Ewert, F. (2013). Global hot-spots of heat stress on agricultural crops due to climate change. *Agricultural and Forest Meteorology*, *170*, 206–215.https://doi.org/10.1016/j.agrformet.2011.09.002

Tormena, C. A., da Silva, A. P., & Libardi, P. L. (1999). Soil physical quality of a Brazilian Oxisol under two tillage systems using the least limiting water range approach. *Soil and Tillage Research*, *52*, 223–232.https://doi.org/10.1016/S0167-1987(99)00086-0

van Lier, Q. d. J., & Gubiani, P. I. (2015). Beyond the "least limiting water range": Rethinking soil physics research in Brazil. *Revista*

Brasileira de Ciência do Solo, *39*, 925–939.https://doi.org/10.1590/01000683rbcs20140596

Wesseling, J., & Van Wijk, W. (1957). Soil physical conditions in relation to drain depth. In J. N. Luthin (Ed.), *Drainage of agricultural lands* pp. 461–504). Madison, WI: ASA.

Whitmore, A. P., & Whalley, W. R. (2009). Physical effects of soil drying on roots and crop growth. *Journal of Experimental Botany*, *60*, 2845–2857.https://doi.org/10.1093/jxb/erp200

Williams, J., Ross, P., & Bristow, K. L. (1989). Prediction of the Campbell water retention function from texture, structure, and organic matter. In M. Th. van Genuchten & F. J. Leij (Eds.), *Proceedings of the international workshop on indirect methods for estimating the hydraulic properties of unsaturated soils* (pp. 427–441). Canberra: CSIRO.

Zou, C., Sands, R., Buchan, G., & Hudson, I. (2000). Least limiting water range: A potential indicator of physical quality of forest soils. *Soil Research*, *38*, 947–958.https://doi.org/10.1071/SR99108

SUPPORTING INFORMATION

Additional supporting information may be found online in the Supporting Information section at the end of the article.

How to cite this article: Pulido-Moncada M, Petersen CT, Munkholm LJ. Limiting water range: Crop responses related to in-season soil water dynamics, weather conditions, and subsoil compaction. *Soil Sci Soc Am J*. 2021;1–17. https://doi.org/10.1002/saj2.20174